

Overexpression of the cholesterol-binding protein MLN64 induces liver damage in the mouse

Juan Enrique Tichauer, María Gabriela Morales, Ludwig Amigo, Leopoldo Galdames, Andrés Klein, Verónica Quiñones, Carla Ferrada, Alejandra Alvarez R, Marie-Christine Rio, Juan Francisco Miquel, Attilio Rigotti, Silvana Zanlungo

Juan Enrique Tichauer, María Gabriela Morales, Ludwig Amigo, Leopoldo Galdames, Andrés Klein, Verónica Quiñones, Carla Ferrada, Juan Francisco Miquel, Attilio Rigotti, Silvana Zanlungo, Departamento de Gastroenterología, Facultad de Medicina, Pontificia Universidad Católica, Santiago, Chile

Alejandra Alvarez R, Departamento de Biología Celular y Molecular, Facultad de Ciencias Biológicas, Pontificia Universidad Católica, Santiago, Chile

Marie-Christine Rio, Institut de Génétique et de Biologie Moléculaire et Cellulaire, INSERM U596, 67404 Illkirch, France
Supported by Fondo Nacional de Desarrollo Científico y Tecnológico, FONDECYT grant No. 1030415 to S.Z. and No. 1030416 to A.R.

Correspondence to: Dr. Silvana Zanlungo, Pontificia Universidad Católica de Chile, Departamento de Gastroenterología, Marcoleta 367, Santiago, Chile. silvana@med.puc.cl
Telephone: +56-2-6863820 Fax: +56-2-6397780
Received: 2007-02-27 Accepted: 2007-03-28

Abstract

AIM: To examine the *in vivo* phenotype associated with hepatic metastatic lymph node 64 (MLN64) overexpression.

METHODS: Recombinant-adenovirus-mediated MLN64 gene transfer was used to overexpress MLN64 in the livers of C57BL/6 mice. We measured the effects of MLN64 overexpression on hepatic cholesterol content, bile flow, biliary lipid secretion and apoptosis markers. For *in vitro* studies cultured CHO cells with transient MLN64 overexpression were utilized and apoptosis by TUNEL assay was measured.

RESULTS: Livers from Ad.MLN64-infected mice exhibited early onset of liver damage and apoptosis. This response correlated with increases in liver cholesterol content and biliary bile acid concentration, and impaired bile flow. We investigated whether liver MLN64 expression could be modulated in a murine model of hepatic injury. We found increased hepatic MLN64 mRNA and protein levels in mice with chenodeoxycholic acid-induced liver damage. In addition, cultured CHO cells with transient MLN64 overexpression showed increased apoptosis.

CONCLUSION: In summary, hepatic MLN64 overexpression induced damage and apoptosis in murine

livers and altered cholesterol metabolism. Further studies are required to elucidate the relevance of these findings under physiologic and disease conditions.

© 2007 The WJG Press. All rights reserved.

Key words: Metastatic lymph node 64; Apoptosis; Cholesterol; Liver; StarD3

Tichauer JE, Morales MG, Amigo L, Galdames L, Klein A, Quiñones V, Ferrada C, Alvarez AR, Rio MC, Miquel JF, Rigotti A, Zanlungo S. Overexpression of the cholesterol-binding protein MLN64 induces liver damage in the mouse. *World J Gastroenterol* 2007; 13(22): 3071-3079

<http://www.wjgnet.com/1007-9327/13/3071.asp>

INTRODUCTION

MLN64 (metastatic lymph node 64) cDNA was originally discovered as a highly expressed and amplified gene in certain breast, gastric, and esophageal cancers^[1-3]. Although MLN64 could play a causative role in tumorigenesis, its amplification probably reflects the close genomic proximity (within 36 kb) to the oncogene *c-erb-B2* (*her-2/neu*), which is invariantly coamplified^[3,4]. The N-terminal of MLN64, the so-called MENTAL domain, includes four transmembrane helices, whereas the C-terminal domain contains the StAR-related lipid transfer domain (START)^[5,6]. The latter domain is present in proteins involved in diverse cell functions^[6,7] and exhibits 37% identity with StAR^[5,6]. There is a family of proteins with homology to StAR, each containing the 200-210-aa START domain, in which MLN64 is known as StarD3^[5,6].

Like StAR, the isolated MLN64 START domain binds^[5] and transfers^[8] cholesterol *in vitro* to the mitochondria and stimulates steroidogenesis when cotransfected with the cytochrome P450_{scc}^[8,9]. However, full-length MLN64 is less active in steroidogenic assays since its transmembrane domain localizes it to late endosomes with the START domain facing the cytosol^[8,10]. For this reason, the role of MLN64 in steroidogenesis is still unclear, but it has been suggested that proteolysis could release the START domain to allow delivery of cholesterol to mitochondria^[8]. This putative role for MLN64 in steroidogenesis has led to

speculation that high levels of MLN64 observed in some breast carcinomas could contribute to the progression of these tumors through increased intratumoral steroidogenesis^[4].

The localization and topology of MLN64 in late endosomes suggest that this protein participates in the efflux of cholesterol from late endosomes and lysosomes, possibly together with other proteins such as Niemann-Pick type C (NPC)1 and NPC2^[10,11]. NPC disease is a lysosomal cholesterol-storage neurodegenerative disorder that is caused by deficiency of either NPC1 or NPC2^[12,13]. Interestingly, expression of a truncated MLN64 protein lacking the START domain caused accumulation of free cholesterol in lysosomes of COS-1 and CHO cells, causing an NPC-like cellular phenotype^[8]. These results suggest that MLN64 plays a role in the maintenance of endosomal cholesterol flow and intracellular cholesterol homeostasis. However, the overexpression of full-length MLN64 also induced an increase in sterol accumulation in COS cells, arguing against a role for MLN64 in cholesterol efflux from this compartment^[14]. Moreover, mice with targeted mutation of the MLN64 START domain were neurologically intact and fertile, and exhibited only modest alterations in cellular sterol metabolism^[15], leaving unanswered the question of MLN64 function *in vivo*.

MLN64 expression is detected in all tissues^[16]. In the liver, MLN64 could mobilize cholesterol into mitochondria where it should be oxidized in the first step of the acidic pathway for bile acid synthesis^[17]. Indeed, Pandak *et al*^[18] and Ren *et al*^[19,20] demonstrated that overexpression of the closest homologue of MLN64 in liver cells, StAR, leads to an important increase in bile acid synthesis both *in vitro* and *in vivo*. However, MLN64 overexpression in primary rat hepatocytes produced only a 20% increase in the rate of bile acid synthesis, suggesting that the hepatic expression of this protein is not a major determinant of the transport of cholesterol to the mitochondria during bile acid synthesis^[19].

Even though MLN64 has been suggested to participate in intracellular cholesterol mobilization and steroidogenesis, its physiological function remains unclear. Interestingly, MLN64 cDNA has also been associated with other cellular processes such as the actin-mediated dynamics of late endocytic organelles^[14] and apoptosis, since a differential-display analysis identified the gene as being downregulated in retinoic acid-induced apoptosis in T-cell lymphoma^[21]. In the present study, we studied the *in vivo* phenotype associated with MLN64 overexpression in liver using an adenovirus-mediated overexpression strategy. We found that mice with hepatic MLN64 overexpression exhibited significant liver damage and apoptosis, and some minor alterations to cholesterol metabolism.

MATERIALS AND METHODS

Animals and diets

C57BL/6J mice originally purchased from Jackson Laboratory (Bar Harbor, ME) were bred to generate our own colony. All mice had free access to water and a chow diet (< 0.02% cholesterol; Prolab RMH 3000, PMI

Table 1 Primers for gene expression analysis in MLN64-overexpressing mouse livers

Gene	Primers	Fragment size
<i>bax</i>	TATTGGTGAGTCGGATTGC (S) TGGACGGTCAGTGTCTGG (AS)	230 bp
<i>mdm2</i>	CCAACATGTCTGTGTCTACCG (S) ACAATGTGCTGCTGCTTCTC (AS)	216 bp
<i>mln64</i>	TCGACATCTTTGTCTGGCT (S) GAGCAACTCAGAAAGGATGAC (AS)	148 bp
18 S	GTAACCCGTGAACCCATT (S) CCATCCAATCGGTAGTAGCG (AS)	151 bp

S: sense; AS: antisense.

Feeds, St. Louis, MO). In some experiments, 2-mo-old C57BL/6J mice were fed chow supplemented with 2% chenodeoxycholic acid (CDCA) for 1 or 2 d.

Protocols were performed according to accepted criteria for the humane care of experimental animals, and were approved by the review board for animal studies of our institution.

Preparation and administration of recombinant adenoviruses

The recombinant adenovirus encoding the full-length murine MLN64 cDNA (Ad.MLN64), under control of the cytomegalovirus (CMV) promoter, was generated by homologous recombination in bacterial cells using the AdEasy system (generously provided by Dr. Bert Vogelstein, The Johns Hopkins University, Baltimore, MD)^[22]. The control adenovirus Ad.E1Δ, containing no transgene, was kindly donated by Dr. Karen Kozarsky (SmithKline Beecham Pharmaceuticals, King of Prussia, PA). Large-scale production of recombinant adenoviruses was performed from infected HEK 293 cells as described previously^[23].

For viral administration, mice of 2 mo-old were anesthetized by ether inhalation, the femoral vein was exposed, and 1x10¹¹ viral particles (in 0.1 mL of isotonic saline buffer) of control or recombinant adenoviruses were injected intravenously. An additional control group received 0.1 mL of saline buffer only. Animals were studied 12-24 h after adenoviral infection.

Gene expression analysis by semiquantitative RT-PCR

Five micrograms of total liver RNA from individual animals was reverse transcribed using random hexamer primers. Semiquantitative RT-PCR was performed in the presence of [α -³²P]dCTP for *bax* and *mdm2* genes using primers based on mouse and rat cDNA sequences available in GeneBank databases (Table 1). After an initial 5 min 94°C denaturation step, thermal cycling involved 28 cycles at 94°C for 30 s, 52°C for 30 s, and 72°C for 30 s for *bax* mRNA analysis and 29 cycles at 94°C for 1 min, 52°C for 1 min, and 72°C for 1 min for *mdm2* mRNA analysis.

Gene expression levels were compared to coamplification of 18S internal standards (Ambion, Austin, TX). PCR products were resolved by 2% agarose gel electrophoresis and transferred to a nylon filter.

Radiolabeled bands were quantified using an imaging system (Molecular Imager GS-525, BIO-RAD, Hercules, CA), with the results normalized to the signal generated by radiolabeled 18S PCR products.

MLN64 gene expression analysis by real-time PCR

Two micrograms of total RNA from each liver sample were pretreated with DNase I (Invitrogen, Carlsbad, CA) to remove any contaminating genomic DNA, and then reverse-transcribed to cDNA with random hexamers (Invitrogen, Carlsbad, CA). Real-time PCR was performed with a Stratagene Mx3000P Real-Time PCR System and Brilliant SYBR Green QPCR Master Mix (Stratagene, La Jolla, CA) using 50 ng cDNA per 20 μ L reaction volume, a SYBR green master mix and *mln64*-specific primers (Table 1). Changes in gene expression for *mln64* were determined and normalized to 18S rRNA expression levels.

Immunoblotting analysis

For MLN64, total membrane extracts and 10 000 \times g mitochondria/lysosome enriched-pellets from murine liver were prepared^[24], and proteins were fractionated by 10% SDS-PAGE. After transfer to nitrocellulose, proteins were immunoblotted for MLN64 using anti-MLN64 antiserum^[10] and a commercial antibody ab3478 (Abcam, Cambridge, UK). An anti- ϵ -COP (Coatomer Protein Complex Subunit Epsilon) antibody (obtained from Dr. Monty Krieger, Massachusetts Institute of Technology, Cambridge, MA) was used as a control for the membrane protein loading.

Liver homogenates were prepared for analyzing p53, p21, and Bax protein expressions^[25]. For caspase-3 and -12 immunoblotting, liver homogenates were fractionated into total membranes and cytosol as described previously^[23]. Proteins (50 μ g/sample) were separated by 12% SDS-PAGE and immunoblotted using anti-caspase-12 (BD Biosciences Pharmingen, San Diego, CA), anti-caspase-3, anti-p53, anti-p21 and anti-Bax (Santa Cruz Biotechnology, Santa Cruz, CA). An anti-albumin antibody was used for protein normalization.

Antibody binding to protein samples was visualized using enhanced chemiluminescence and measured using an imaging system (Molecular Imager GS-525, BIO-RAD).

Bile, liver, and blood sampling

Mice were anesthetized by intraperitoneal injection of sodium pentobarbital. After laparotomy, the cyst duct was ligated and a fistula was made in the common bile duct using a polyethylene catheter. Hepatic bile specimens were collected for 30 min, then plasma and liver samples were obtained as described previously^[26,27].

Plasma, hepatic, and biliary biochemical analyses

Serum alkaline phosphatase (AP) and alanine aminotransferase (ALT) were measured by standard methods. Hepatic and biliary cholesterol as well as biliary phospholipids and bile acids were determined by standard protocols^[28,29].

Hepatic immunofluorescence

Fresh-frozen liver tissues cryosectioned at 4–5 μ m were

fixed in acetone, rinsed three times in phosphate-buffered saline (PBS), permeabilized with 0.1% Triton X-100 for 15 min, blocked overnight in 10% goat serum in PBS, and incubated for 2 h at 37°C with the polyclonal antibody against MLN64 (1:500 dilution). The secondary antibody was fluorescein-isothiocyanate-conjugated goat antirabbit IgG (1:150 dilution). After washing in PBS, samples were mounted on coverslips using Fluoromount-G (EMS, Fort Washington, MD). Stained sections were examined by immunofluorescence microscopy.

Hepatic histology

Liver tissue was fixed in 4% paraformaldehyde for 48 h and then embedded in paraffin, sectioned, and placed on glass slides. Hematoxylin and eosin staining was then performed according to standard procedures.

Hepatic TUNEL analysis

TUNEL (TdT-mediated dUTP nick end labeling) staining was performed on sections of liver samples using a commercially available kit (TUNEL Apoptosis Detection Kit, Upstate, Charlottesville, VA) according to the manufacturer's recommendations with minor modifications. Briefly, cryosections of fresh-frozen tissues were fixed in 4% paraformaldehyde in PBS for 30 min at room temperature. The tissue was permeabilized with 0.1% Triton X-100 and 0.1 mol/L sodium acetate for 2 min at 4°C, and then washed twice with PBS. Tissues were subjected to proteinase K treatment for 15 min. The DNA of apoptotic cells was enzymatically labeled with the terminal deoxynucleotidyl transferase for 1 h at 37°C and visualized by staining with fluorescein.

Hepatic DNA fragmentation analysis

Liver tissue samples were lysed with hypotonic lysis buffer (50 mmol/L EDTA, 1% SDS, 50 mg/L proteinase K in 50 mmol/L Tris-HCl, pH 8) for 15 min on ice, and then incubated for 4 h at 37°C. DNA was extracted with an equal volume of phenol/chloroform followed by chloroform isoamylalcohol (24:1) extraction, the aqueous phase was collected, and DNA was precipitated by adding 150 mmol/L sodium acetate and two volumes of ethanol at -20°C for 1 h. The precipitate was pelleted by centrifugation at 10 000 \times g, and then washed in cold 70% ethanol. After centrifugation, each pellet was dissolved in autoclaved distilled water and electrophoresed on a 1.5% agarose gel containing 2 μ g/mL ethidium bromide. DNA fragments were visualized in an ultraviolet transilluminator.

Cell culture and transfections, TUNEL staining, and Hoechst analysis

Chinese hamster ovary (CHO)-K1 cells were grown in Ham F-12 media supplemented with 10% fetal bovine serum (FBS), 100 μ g/mL streptomycin, and 100 U/mL penicillin and maintained at 37°C, in an atmosphere of 5% CO₂, and saturated humidity. CHO cells were transfected using a lipofectAMINE 2000 reagent (Invitrogen, Carlsbad, CA) with a pcDNA3.1 empty plasmid or a pcDNA3.1/MLN64 vector that was constructed by ligation of a cDNA HindIII fragment encoding mouse

MLN64 in pcDNA3.1 (Invitrogen, Carlsbad, CA). After 24 h cells were subjected to immunofluorescence, TUNEL analysis, and Hoechst staining.

For immunofluorescence, CHO cells were fixed in 4% paraformaldehyde in PBS for 1 h, permeabilized with 0.1% Triton X-100/0.1% sodium citrate in PBS for 2 min, blocked 20 min in 0.02% gelatin in PBS and incubated 2 h with anti-MLN64 ab3478 antibodies (Abcam, Cambridge, UK) at 1:1000 dilution, followed by incubation with a Alexa-594-conjugated goat anti-rabbit IgG (Molecular Probes, Eugene, OR, dilution 1:1000). TUNEL analysis was performed using a commercial kit following manufacturer's recommendations (Roche, Mannheim, Germany). For Hoechst 33258 staining, cells were incubated with 1:50 000 dilution of Hoechst 33258 (Polysciences, Warrington, Pennsylvania) for 15 min at 37°C. Fluorescence was analyzed and photographed under an appropriate microscope (Olympus BX51 TF, Tokyo, Japan).

Statistical analysis

Results are expressed as mean \pm standard error values. The statistical significance of differences between the means of the experimental groups was evaluated using Student's *t*-test for unpaired data and with one-way analysis of variance (ANOVA) with a post-hoc Tukey multiple-comparison test (Prism 3.0, GraphPad). A difference was considered statistically significant when the probability value was $P < 0.05$.

RESULTS

Hepatic MLN64 expression and localization in recombinant MLN64 adenovirus-infected mice

To determine the effects of hepatic MLN64 overexpression, Ad.MLN64 and the control Ad.E1 Δ were infected into C57BL/6 mice. Western blot analysis (Figure 1A) of mitochondria/lysosome enriched preparations demonstrated that MLN64 protein was increased several times in the livers of Ad.MLN64-treated C57BL/6 mice at 24 h after infection. Overexpressed MLN64 was detected as a predominant 50-kDa protein^[16]. The increase in hepatic MLN64 protein levels induced by the infusion of Ad.MLN64 was time-dependent (Figure 1B), reaching its maximal effect after 24 h of infection, and decreasing to undetectable levels after 96 h. Thus, all the subsequent experiments were performed at 24 h after Ad.MLN64 infection.

The liver MLN64 staining was essentially intracellular in Ad.MLN64-infected mice, exhibiting an abundant punctate pattern (Figure 1C) consistent with MLN64 protein localization in vesicular compartments as reported previously in other cell types^[8,10].

Liver damage and apoptosis in mice with adenovirus-mediated hepatic MLN64 overexpression

As described above, hepatic MLN64 expression was highly increased at 12-24 h after infection with Ad.MLN64, but it dramatically decreased 96 h thereafter (Figure 1). This short half-life for transgene expression is an unusual

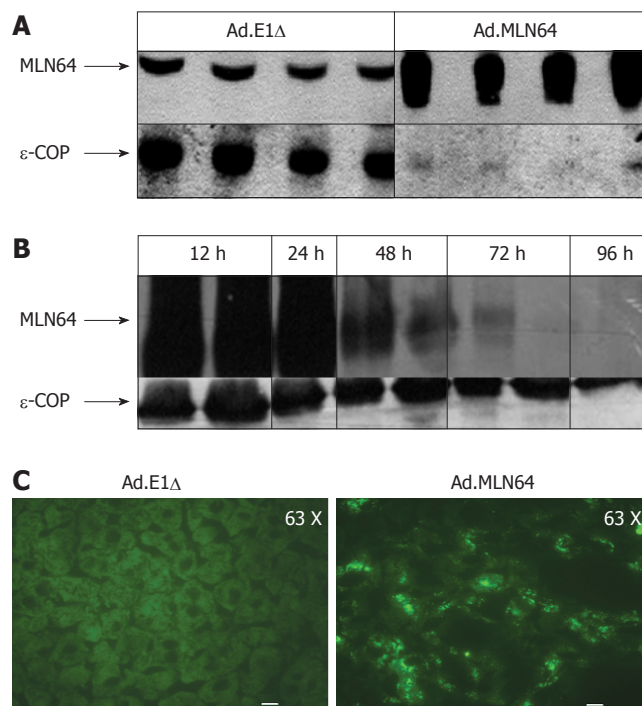


Figure 1 Effect of recombinant MLN64 adenovirus infection on MLN64 expression in mice livers. **A:** Immunoblot analysis of MLN64. At 24 h after infection, mitochondria/lysosome enriched extracts (50 μ g protein/lane from Ad.E1 Δ and 1 μ g protein/lane from Ad.MLN64 mouse livers) were subjected to 10% SDS-PAGE and Western blotting with anti-MLN64 and anti- ϵ -COP antibodies; **B:** Time course of hepatic MLN64 expression after administration of recombinant adenovirus. At the indicated times (in hours) after infection, livers were collected and analyzed for MLN64 protein expression in total membrane extracts as described in (A); **C:** Immunofluorescence analysis of liver tissue 24 h after infection with control (Ad.E1 Δ) or MLN64 (Ad.MLN64) recombinant adenovirus. Bar: 10 μ m. Analysis were performed in four mice in each experimental group. Results are representative of three independent experiments.

finding for adenovirus-mediated gene expression in the liver, given that both previous studies^[30,31] and our own investigations have found substantial levels of protein expression for other genes using this type of adenovirus still at 2 wk after infection.

To explore the potential mechanisms underlying the rapid decrease in MLN64 overexpression, we evaluated liver damage and apoptosis in MLN64-infected mice. The first evidence of hepatic damage in these animals was in the gross morphology of the liver, with the formation of yellowish-white zones suggesting the presence of hepatic necrosis at 24 h after infection (Figure 2A). Furthermore, serum ALT and AP were significantly elevated in mice infected with virus-encoding CMV-MLN64 compared with both noninfected mice and those infected with the control Ad.E1 Δ virus (Table 2). Interestingly, we found a dose-effect response in serum ALT and AP levels utilizing lower doses of viral particles (results not shown). Histological examination of liver sections demonstrated the presence of multiple necrotic zones as well as numerous condensed and fragmented nuclei, which are characteristic of apoptosis (Figure 2B). DNA fragmentation analysis and TUNEL assays revealed the presence of a DNA "ladder" pattern and TUNEL-positive cells in livers of MLN64-overexpressing mice (Figure 3), confirming that the

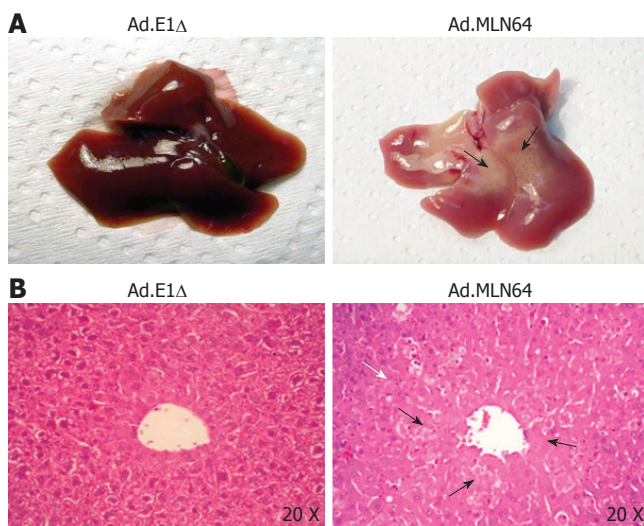


Figure 2 Effect of recombinant MLN64 adenovirus infection on liver morphology and histology in mice. **A:** Gross morphology of murine livers 24 h after infection with Ad.E1 Δ or Ad.MLN64. Arrows indicate yellowish-white zones with liver necrosis in Ad.MLN64-infected mice; **B:** Liver sections from (A) were prepared for histology and stained with hematoxylin and eosin. Small arrows indicate necrotic zones, and the white arrow indicates an apoptotic zone. Analysis were performed in four mice in each experimental group. Results are representative of three independent experiments.

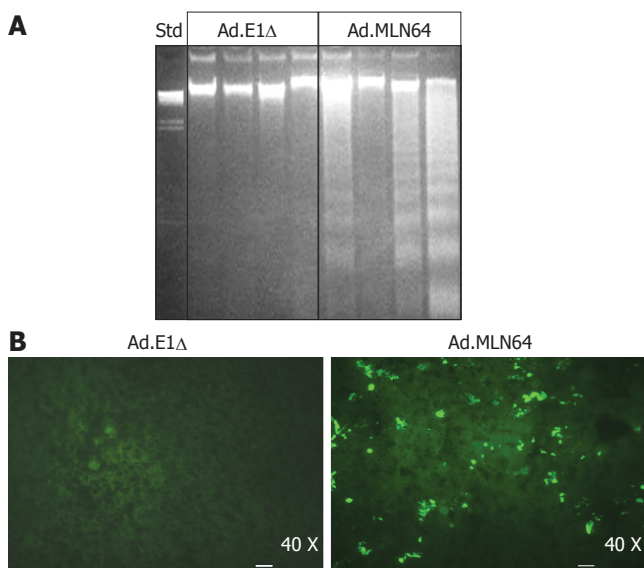


Figure 3 Effect of recombinant MLN64 adenovirus infection on liver apoptosis in mice. DNA fragmentation analysis and TUNEL assay were performed in murine livers 24 h after infection with Ad.E1 Δ or Ad.MLN64 as biochemical markers of apoptosis. **A:** DNA fragmentation analysis of liver tissue by DNA agarose gel electrophoresis. DNA λ /Hind III was used as the standard (Std); **B:** TUNEL assay. Substantially more apoptotic cells were detected in liver sections from Ad.MLN64-infected mice than in those from Ad.E1 Δ -infected mice. Analysis were performed in four mice in each experimental group. Results are representative of three independent experiments.

apoptosis was induced by MLN64 overexpression.

The acute hepatocyte apoptosis/necrosis induced by MLN64 overexpression was fully reversible, with livers appeared healthy and normal at 1 wk after Ad.MLN64 infection, when no MLN64 expression was detected (data not shown). Remarkably, mortality was not increased in

Table 2 Effects of MLN64 recombinant adenoviral infection on serum alanine aminotransferase and alkaline phosphatase (mean \pm SE)

Group	ALT U/L	AP U/L
No virus	14.00 \pm 7.04	55.25 \pm 6.44
Ad.E1 Δ	39.67 \pm 4.91	76.33 \pm 4.42
Ad.MLN64	3780 \pm 1010 ^a	209.50 \pm 20.17 ^a

Measurements were performed in four mice in each experimental group. ^a*P* < 0.05 vs Ad.E1 Δ -infected mice.

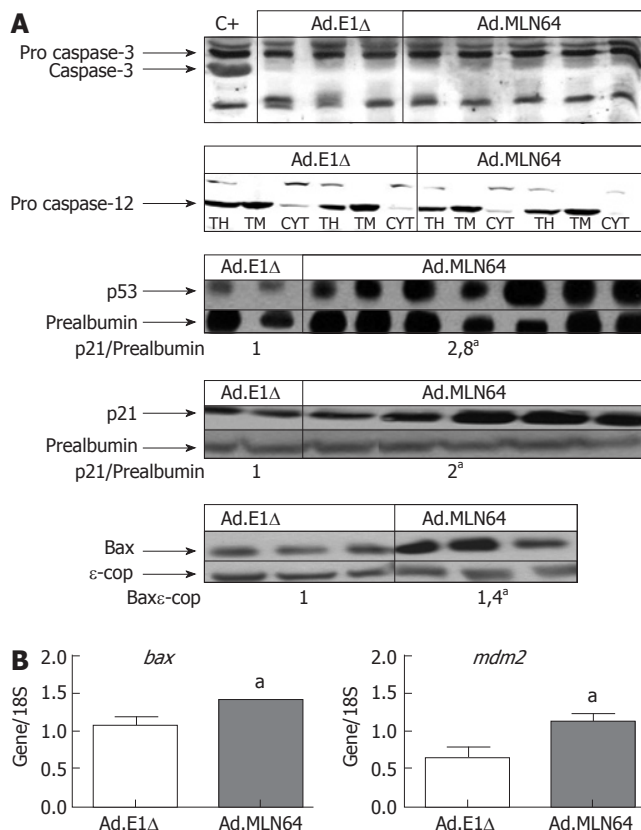


Figure 4 Effect of recombinant MLN64 adenovirus infection on hepatic expressions of various apoptosis-regulating genes in mice. **A:** For caspase-3 analysis, liver cytosolic fractions were prepared from Ad.MLN64-infected mice, and a liver cytosolic fraction from a CDCA-fed mouse was used as a positive control (C+). For caspase-12 analysis, liver homogenates (TH) from two mice in each group were fractionated into total membranes (TM) and cytosol (CYT). Total liver extracts were prepared for the analysis of p53, p21, and Bax expressions. Proteins were size fractionated by SDS-PAGE, immunoblotted with anti-caspase-3, anti-caspase-12, anti-p53, anti-p21, and anti-Bax antibodies, and subjected to densitometric analysis. The protein expression data are shown after normalization to the ϵ -COP or albumin signal. ^a*P* < 0.05; **B:** Relative quantitative RT-PCR in the presence of [α -³²P]dCTP was used to analyze the *bax* and *mdm2* RNA expressions. A 18S primer control was included in each sample. The products were resolved on a 1.5% agarose gel and transferred to a nylon filter, and the radiolabeled signals were quantified. Results are representative of three independent experiments. ^a*P* < 0.05.

Ad.MLN-64-infected mice compared to controls.

To further clarify the mechanism of MLN64-induced apoptosis, we evaluated the hepatic expressions of various apoptosis-related genes (Figure 4). Western blot analysis in MLN64-overexpressing mice revealed a significant increase in the expressions of proapoptotic proteins p53,

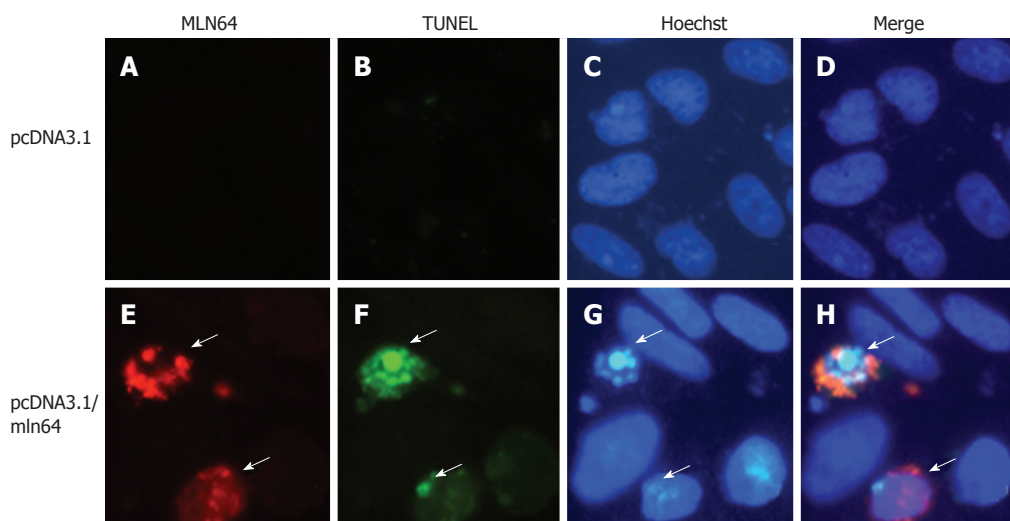


Figure 5 Effect of MLN64 overexpression on apoptosis in CHO cells. CHO-K1 cells were transfected with a pcDNA3.1 empty or a pcDNA3.1/MLN64 vector, analyzed by MLN64 immunofluorescence (A, E), TUNEL (B, F), or Hoechst 33258 (C, G) staining, and visualized under fluorescence microscopy. Merge of panels A, B and C and E, F and G are shown in panels D and H. Arrows indicate MLN64 overexpressing cells.

Table 3 Effects of MLN64 recombinant adenoviral infection on hepatic cholesterol levels, biliary bile flow, and lipid secretion (mean ± SE)

Group	Liver weight	Hepatic cholesterol		Bile flow ($\mu\text{L}/\text{min}/100\text{ g}$ body weight)	Biliary lipid secretion		
		Unesterified (mg/g liver weight)	Ester (mg/g liver weight)		Cholesterol (nmol/min/100 g body weight)	Bile salts (nmol/min/100 g body weight)	Phospholipids (nmol/min/100 g body weight)
Ad.E1 Δ	1.32 ± 0.04 (n = 11)	1.97 ± 0.08	0.20 ± 0.08	9.43 ± 0.76 (n = 8)	2.75 ± 0.33	254.1 ± 34.2	84.25 ± 5.5
Ad.MLN64	1.14 ± 0.04 (n = 16) ^a	2.38 ± 0.08 ^a	0.21 ± 0.07	4.14 ± 0.61 ^a	1.38 ± 0.19 ^a	308.5 ± 45.4	54.64 ± 13.5

Measurements were performed in six mice in each experimental group, except for liver weight and bile flow as indicated. ^aP < 0.05 vs Ad.E1 Δ -infected mice.

p21, and Bax, whereas the activated forms of caspase-3 and caspase-12 were not detected (Figure 4A). Semiquantitative PCR analysis revealed that *bax* and *mdm2* mRNA levels were increased in MLN64-overexpressing mice (Figure 4B).

Apoptosis in CHO cells with transient MLN64 overexpression

To determine if overexpression of MLN64 in cultured cells, by a system that does not use an adenovirus to overexpress the protein, directly results in increased apoptosis, we transiently transfected CHO-K1 cells and analyzed apoptosis by TUNEL and Hoechst staining. We observed a clear increase in TUNEL positive cells in MLN64-overexpressing cells (Figure 5). Furthermore, nuclear morphology assessed by Hoechst staining of these cells confirmed an ongoing apoptotic process with brightly stained nucleus and chromatin condensation (Figure 5). The percentage of MLN64 transfected CHO cells undergoing apoptosis was 32%, whereas no positive TUNEL cells were detected in control CHO transfected cells with pcDNA3.1. Similar results were obtained in HEK 293 cells with MLN64 transient overexpression (results not shown). These results support a potential role for MLN64 in determining cell death.

Hepatic cholesterol content in mice with adenovirus-mediated hepatic MLN64 overexpression

Since excess cellular free cholesterol is a potent inducer of cell apoptosis^[32,33], and MLN64 overexpression in COS

cells causes cholesterol accumulation^[14], we determined the hepatic total and unesterified cholesterol levels in mice with adenovirus-mediated hepatic MLN64 overexpression. As indicated in Table 3, MLN64 overexpression increased the hepatic free-cholesterol content by 21% relative to control animals.

MLN64 expression in a murine model of liver damage induced by chenodeoxycholic acid

To begin to explore the pathophysiological relevance of our findings, we analyzed MLN64 liver expression in cholestatic hepatocyte injury induced by a diet high in CDCA, which is a well-characterized model of apoptosis-related liver damage induced by bile acids^[34,35]. Figure 6 shows that MLN64 mRNA and protein levels increased significantly compared to control levels, demonstrating that MLN64 expression is indeed modulated in a liver-damage model involving apoptosis.

Biliary lipid secretion in mice with adenovirus-mediated hepatic MLN64 overexpression

Since the phenotype of MLN64-infected mice-including liver damage, apoptosis, and the increase in plasma AP levels-suggested that animals were in a cholestatic condition, we studied the effects of hepatic MLN64 overexpression on bile flow and biliary lipid secretion (Table 3). The total bile flow decreased by 56% in Ad.MLN64-infected mice. The biliary output of cholesterol decreased by approximately 46% and biliary phospholipid secretion showed a trend to decrease. Biliary

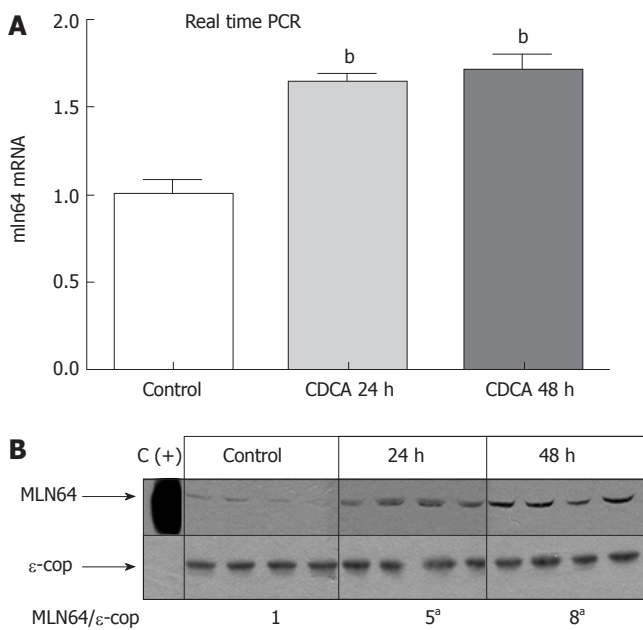


Figure 6 Effect of a 2% CDCA diet on hepatic MLN64 mRNA and protein levels in mice. Mice were fed with a 2% CDCA diet for 1 or 2 d. **A:** Real time PCR was used to analyze *mln64* RNA expression. Each value represents the mean \pm SE for mRNA values determined in CDCA-fed mice relative to those measured in chow diet-fed mice. There were 5 mice in each group. ^b $P < 0.0001$; **B:** Immunoblot analysis of MLN64. Mitochondria-enriched liver extracts (50 μ g protein/lane) were subjected to 10% SDS-PAGE and Western blotting with anti-MLN64 and anti- ϵ -COP antibodies. A liver membrane fraction from an Ad.MLN64-infected mouse was used as a positive control (C+). ^a $P < 0.05$.

bile acid secretion remained within normal range, with a trend to increase. Consistent with the decrease in bile flow without changes in biliary bile acid output, biliary bile acid concentrations were increased twofold in Ad.MLN64-infected mice (71.07 ± 7.2 mmol/L in Ad.MLN64 mice *vs* 35.33 ± 7.4 mmol/L in Ad.E1 Δ mice). The bile acid pool size and composition remained unchanged in Ad.MLN64-infected mice (data not shown).

DISCUSSION

This study demonstrates that adenovirus-mediated MLN64 overexpression in the mouse liver induces liver damage, most likely due to activation of the apoptosis cascade. Consistent with acute and reversible hepatocyte apoptosis induced by MLN64 overexpression, mortality was not increased and livers appeared healthy 7 d after Ad.MLN64 infection when no MLN64 overexpression was detected. In addition, MLN64 hepatic overexpression was associated with changes in hepatic cholesterol content, bile flow, and biliary bile acid concentration.

The precise function of MLN64 is unknown. The MENTAL region of MLN64, which contains four transmembrane domains, associates this protein with the membrane of endosomal compartments^[10], and its C-terminal START domain makes it capable of mobilizing cholesterol^[8,10]. Removal of the MLN64 N-terminal region increased steroidogenesis in COS-1 transfected cells^[16] and enhanced the generation of steroid hormone by placental mitochondria in *in vitro* assays^[8]. However, mice

with targeted mutation of the MLN64 START domain did not exhibit a sterol-metabolism-related phenotype^[15], questioning the physiological importance of the MLN64 START domain in cholesterol trafficking and metabolism.

The most significant finding of our study was the dramatic induction of liver damage in MLN64-infected mice, mainly through apoptosis as demonstrated by both TUNEL and DNA fragmentation analyses. We also detected an increase in ALT and AP plasma levels at 24 h after Ad.MLN64 infection, which is consistent with the current understanding of liver cell apoptosis; it is not a silent process and may also trigger liver inflammation and necrosis^[36]. Adenovirus-mediated MLN64 overexpression was concentrated in some zones of the liver (results not shown). This was correlated with the visualization of hepatic damage in specific zones of the liver and suggests that acute and complete MLN64 down-regulation occurs mainly by apoptosis only in cells overexpressing MLN64. This response should induce liver regeneration in the injured zones and could explain that livers appear healthy 7 d after Ad.MLN64-infection.

We detected an increase in the hepatic levels of p53, p21, Bax, and Mdm2, suggesting that the apoptosis affects various signaling pathways. Surprisingly, active caspase-3 levels were not increased in MLN64-overexpressing livers. Caspase-3 is one of the central effector caspases when apoptosis is initiated by a variety of stimuli^[37], and caspase-3 activation in liver has been described in several models of damage, such as iron deposition, steatohepatitis, and treatment with hepatocarcinogens^[38,39]. The failure to detect caspase-3 activation in the present study could be due to a very low number of cells undergoing apoptosis or a low sensitivity of the caspase-3 antibody, or both. Alternatively, MLN64 overexpression may have induced apoptosis through non-caspase-3-mediated pathways.

The actual mechanism by which MLN64 mediates apoptosis is not clear and requires further study. Examination of the activation of other caspases, such as caspase 6, 7, 8, 9 and 10 should help elucidate is the observed apoptosis is caused by the intrinsic pathway or extrinsic pathway^[37]. One attractive hypothesis for MLN64-induced apoptosis is that this protein stimulates the delivery of free cholesterol into the endoplasmic reticulum (ER) membrane, triggering protein unfolding^[32]. Consistent with this idea, liver unesterified cholesterol levels were increased and hepatic LDL receptor expression, which is normally controlled by the cholesterol levels in the ER, was downregulated in MLN64-overexpressing mice (results not shown). However, caspase-12, a specific effector that is activated during the ER stress response^[37], was not activated in our MLN64-overexpressing mice. Still, we can not totally exclude a role for the ER stress response in MLN64 overexpression-induced apoptosis given that it has been shown that caspase-12 and caspase 4 are not always required for caspase-dependent ER stress induced-apoptosis^[40]. Another possibility is that the lysosomal pathway of apoptosis^[41] was activated in livers of MLN64-overexpressing mice. In this pathway, which can be activated by death receptors, lipid mediators, and photodamage, lysosomal proteases such as Cathepsin b

(Ctsb) can be released by the lysosomes into the cytosol, where they contribute to the apoptotic cascade upstream of mitochondria^[41]. MLN64 overexpression in the endolysosomal compartment may alter membrane structure and composition so as to favor the lysosomal release of proteases, which leads to apoptosis by activation of mitochondria-dependent apoptotic pathways without caspase-3 involvement. Indeed, it has been shown that MLN64 overexpression induces the formation of enlarged endosomes, an effect probably mediated by its MENTAL domain^[42]. Interestingly, *in vitro* studies involving TNF-treated murine fibrosarcoma cells have shown that Ctsb is responsible for apoptosis-associated changes in the absence of caspase activity^[43]. Further studies using Ctsb-/- mice and Ctsb inhibitors will help to ascertain the importance of lysosomal Ctsb release to this response and whether Ctsb inactivation attenuates the liver damage and apoptosis induced by MLN64 overexpression. Also, additional work is required to determine whether the increase in free-cholesterol levels and the MLN64 subcellular localization are important in the apoptotic response induced by MLN64 overexpression.

Our results using CHO cells with transient MLN64 overexpression supports a role for MLN64 in apoptosis. This cell culture system, which does not use the adenovirus to overexpress itself, is extremely useful in addressing concerns about the amount of adenovirus or adenoviral contaminants as the cause for the hepatotoxic effects. In addition, our results show that MLN64 effect on apoptosis is present in other cell types from diverse origin, such as CHO cells, which are derived from hamster ovary and not only in mouse hepatic-derived cells. We found that 30% of MLN64 overexpressing CHO were undergoing an apoptotic process. This results show that although there is a significant percentage of the population undergoing apoptosis, much higher than in cells that overexpress any protein, not all cells are suffering cell death. This may explain why previous overexpression studies of MLN64 in CHO, COS and HeLa cells and primary rat hepatocytes have not seen an increase in cell death^[8,14,19].

The (patho) physiological relevance of our findings is further supported by the results obtained in mice with CDCA-induced liver injury^[34,35]. In fact, we found a significant increase in hepatic MLN64 protein and mRNA levels in the bile acid-induced liver injury model. This correlative evidence *in vivo* suggested a potential direct role on MLN64 expression in hepatocyte death due to CDCA administration.

MLN64 overexpression also increased the hepatic free-cholesterol content. This finding is consistent with a role for MLN64, proposed by Ren *et al*^[19], in delivering cholesterol from lysosomes to the plasma membrane, where most of the cellular free cholesterol resides^[44]. Another possibility is that cholesterol that accumulates in late endosomes primarily drives MLN64 protein to this subcellular compartment^[14]. Further analyses are required to determine whether increased hepatic free cholesterol in MLN64-infected mice is localized in the plasma membrane or in intracellular compartments, and how this phenomenon is related to the apoptotic process.

In conclusion, we have shown that MLN64 overexpression induces apoptosis in the murine liver and alters cholesterol-metabolism-related parameters. Further studies are required to elucidate the physiological relevance of these findings.

ACKNOWLEDGMENTS

The authors thank Dr. David Cohen and Dr. Flavio Nervi for technical support and helpful discussions.

REFERENCES

- 1 Tomasetto C, Régner C, Moog-Lutz C, Mattei MG, Chenard MP, Lidereau R, Basset P, Rio MC. Identification of four novel human genes amplified and overexpressed in breast carcinoma and localized to the q11-q21.3 region of chromosome 17. *Genomics* 1995; **28**: 367-376
- 2 Akiyama N, Sasaki H, Ishizuka T, Kishi T, Sakamoto H, Onda M, Hirai H, Yazaki Y, Sugimura T, Terada M. Isolation of a candidate gene, CAB1, for cholesterol transport to mitochondria from the c-ERBB-2 amplicon by a modified cDNA selection method. *Cancer Res* 1997; **57**: 3548-3553
- 3 Moog-Lutz C, Tomasetto C, Régner CH, Wendling C, Lutz Y, Muller D, Chenard MP, Basset P, Rio MC. MLN64 exhibits homology with the steroidogenic acute regulatory protein (STAR) and is over-expressed in human breast carcinomas. *Int J Cancer* 1997; **71**: 183-191
- 4 Alpy F, Boulay A, Moog-Lutz C, Andarawewa KL, Degot S, Stoll I, Rio MC, Tomasetto C. Metastatic lymph node 64 (MLN64), a gene overexpressed in breast cancers, is regulated by Sp/KLF transcription factors. *Oncogene* 2003; **22**: 3770-3780
- 5 Tsujishita Y, Hurley JH. Structure and lipid transport mechanism of a StAR-related domain. *Nat Struct Biol* 2000; **7**: 408-414
- 6 Alpy F, Tomasetto C. Give lipids a START: the StAR-related lipid transfer (START) domain in mammals. *J Cell Sci* 2005; **118**: 2791-2801
- 7 Soccio RE, Breslow JL. StAR-related lipid transfer (START) proteins: mediators of intracellular lipid metabolism. *J Biol Chem* 2003; **278**: 22183-22186
- 8 Zhang M, Liu P, Dwyer NK, Christenson LK, Fujimoto T, Martinez F, Comly M, Hanover JA, Blanchette-Mackie EJ, Strauss JF. MLN64 mediates mobilization of lysosomal cholesterol to steroidogenic mitochondria. *J Biol Chem* 2002; **277**: 33300-33310
- 9 Bose HS, Whittal RM, Huang MC, Baldwin MA, Miller WL. N-218 MLN64, a protein with StAR-like steroidogenic activity, is folded and cleaved similarly to StAR. *Biochemistry* 2000; **39**: 11722-11731
- 10 Alpy F, Stoeckel ME, Dierich A, Escola JM, Wendling C, Chenard MP, Vanier MT, Gruenberg J, Tomasetto C, Rio MC. The steroidogenic acute regulatory protein homolog MLN64, a late endosomal cholesterol-binding protein. *J Biol Chem* 2001; **276**: 4261-4269
- 11 Strauss JF, Liu P, Christenson LK, Watari H. Sterols and intracellular vesicular trafficking: lessons from the study of NPC1. *Steroids* 2002; **67**: 947-951
- 12 Carstea ED, Morris JA, Coleman KG, Loftus SK, Zhang D, Cummings C, Gu J, Rosenfeld MA, Pavan WJ, Krizman DB, Nagle J, Polymeropoulos MH, Sturley SL, Ioannou YA, Higgins ME, Comly M, Cooney A, Brown A, Kaneski CR, Blanchette-Mackie EJ, Dwyer NK, Neufelder EB, Chang TY, Liscum L, Strauss JF, Ohno K, Zeigler M, Carmi R, Sokol J, Markie D, O'Neill RR, van Diggelen OP, Elleder M, Patterson MC, Brady RO, Vanier MT, Pentchev PG, Tagle DA. Niemann-Pick C1 disease gene: homology to mediators of cholesterol homeostasis. *Science* 1997; **277**: 228-231
- 13 Naureckiene S, Sleat DE, Lackland H, Fensom A, Vanier MT, Wattiaux R, Jadot M, Lobel P. Identification of HE1 as the second gene of Niemann-Pick C disease. *Science* 2000; **290**: 2298-2301

- 14 **Hölttä-Vuori M**, Alpy F, Tanhuanpää K, Jokitalo E, Mutka AL, Ikonen E. MLN64 is involved in actin-mediated dynamics of late endocytic organelles. *Mol Biol Cell* 2005; **16**: 3873-3886
- 15 **Kishida T**, Kostetskii I, Zhang Z, Martinez F, Liu P, Walkley SU, Dwyer NK, Blanchette-Mackie EJ, Radice GL, Strauss JF. Targeted mutation of the MLN64 START domain causes only modest alterations in cellular sterol metabolism. *J Biol Chem* 2004; **279**: 19276-19285
- 16 **Watari H**, Arakane F, Moog-Lutz C, Kallen CB, Tomasetto C, Gerton GL, Rio MC, Baker ME, Strauss JF. MLN64 contains a domain with homology to the steroidogenic acute regulatory protein (StAR) that stimulates steroidogenesis. *Proc Natl Acad Sci USA* 1997; **94**: 8462-8467
- 17 **Russell DW**. The enzymes, regulation, and genetics of bile acid synthesis. *Annu Rev Biochem* 2003; **72**: 137-174
- 18 **Pandak WM**, Ren S, Marques D, Hall E, Redford K, Mallonee D, Bohdan P, Heuman D, Gil G, Hylemon P. Transport of cholesterol into mitochondria is rate-limiting for bile acid synthesis via the alternative pathway in primary rat hepatocytes. *J Biol Chem* 2002; **277**: 48158-48164
- 19 **Ren S**, Hylemon P, Marques D, Hall E, Redford K, Gil G, Pandak WM. Effect of increasing the expression of cholesterol transporters (StAR, MLN64, and SCP-2) on bile acid synthesis. *J Lipid Res* 2004; **45**: 2123-2131
- 20 **Ren S**, Hylemon PB, Marques D, Gurley E, Bodhan P, Hall E, Redford K, Gil G, Pandak WM. Overexpression of cholesterol transporter StAR increases in vivo rates of bile acid synthesis in the rat and mouse. *Hepatology* 2004; **40**: 910-917
- 21 **Wang KC**, Cheng AL, Chuang SE, Hsu HC, Su IJ. Retinoic acid-induced apoptotic pathway in T-cell lymphoma: Identification of four groups of genes with differential biological functions. *Exp Hematol* 2000; **28**: 1441-1450
- 22 **He TC**, Zhou S, da Costa LT, Yu J, Kinzler KW, Vogelstein B. A simplified system for generating recombinant adenoviruses. *Proc Natl Acad Sci USA* 1998; **95**: 2509-2514
- 23 **Kozarsky KF**, Jooss K, Donahee M, Strauss JF, Wilson JM. Effective treatment of familial hypercholesterolaemia in the mouse model using adenovirus-mediated transfer of the VLDL receptor gene. *Nat Genet* 1996; **13**: 54-62
- 24 **Jokinen EV**, Landschulz KT, Wyne KL, Ho YK, Frykman PK, Hobbs HH. Regulation of the very low density lipoprotein receptor by thyroid hormone in rat skeletal muscle. *J Biol Chem* 1994; **269**: 26411-26418
- 25 **Zanlungo S**, Amigo L, Mendoza H, Miquel JF, Vio C, Glick JM, Rodríguez A, Kozarsky K, Quiñones V, Rigotti A, Nervi F. Sterol carrier protein 2 gene transfer changes lipid metabolism and enterohepatic sterol circulation in mice. *Gastroenterology* 2000; **119**: 1708-1719
- 26 **Amigo L**, Mendoza H, Castro J, Quiñones V, Miquel JF, Zanlungo S. Relevance of Niemann-Pick type C1 protein expression in controlling plasma cholesterol and biliary lipid secretion in mice. *Hepatology* 2002; **36**: 819-828
- 27 **Rigotti A**, Trigatti BL, Penman M, Rayburn H, Herz J, Krieger M. A targeted mutation in the murine gene encoding the high density lipoprotein (HDL) receptor scavenger receptor class B type I reveals its key role in HDL metabolism. *Proc Natl Acad Sci USA* 1997; **94**: 12610-12615
- 28 **Nervi FO**, Del Pozo R, Covarrubias CF, Ronco BO. The effect of progesterone on the regulatory mechanisms of biliary cholesterol secretion in the rat. *Hepatology* 1983; **3**: 360-367
- 29 **Nervi F**, Marinović I, Rigotti A, Ulloa N. Regulation of biliary cholesterol secretion. Functional relationship between the canalicular and sinusoidal cholesterol secretory pathways in the rat. *J Clin Invest* 1988; **82**: 1818-1825
- 30 **Kozarsky KF**, Donahee MH, Rigotti A, Iqbal SN, Edelman ER, Krieger M. Overexpression of the HDL receptor SR-BI alters plasma HDL and bile cholesterol levels. *Nature* 1997; **387**: 414-417
- 31 **Ye X**, Robinson MB, Pabin C, Quinn T, Jawad A, Wilson JM, Batshaw ML. Adenovirus-mediated *in vivo* gene transfer rapidly protects ornithine transcarbamylase-deficient mice from an ammonium challenge. *Pediatr Res* 1997; **41**: 527-534
- 32 **Feng B**, Yao PM, Li Y, Devlin CM, Zhang D, Harding HP, Sweeney M, Rong JX, Kuriakose G, Fisher EA, Marks AR, Ron D, Tabas I. The endoplasmic reticulum is the site of cholesterol-induced cytotoxicity in macrophages. *Nat Cell Biol* 2003; **5**: 781-792
- 33 **Yao PM**, Tabas I. Free cholesterol loading of macrophages induces apoptosis involving the fas pathway. *J Biol Chem* 2000; **275**: 23807-23813
- 34 **Jones BA**, Gores GJ. Physiology and pathophysiology of apoptosis in epithelial cells of the liver, pancreas, and intestine. *Am J Physiol* 1997; **273**: G1174-G1188
- 35 **Higuchi H**, Gores GJ. Bile acid regulation of hepatic physiology: IV. Bile acids and death receptors. *Am J Physiol Gastrointest Liver Physiol* 2003; **284**: G734-G738
- 36 **Higuchi H**, Gores GJ. Mechanisms of liver injury: an overview. *Curr Mol Med* 2003; **3**: 483-490
- 37 **Philchenkov A**. Caspases: potential targets for regulating cell death. *J Cell Mol Med* 2004; **8**: 432-444
- 38 **Ribeiro PS**, Cortez-Pinto H, Solá S, Castro RE, Ramalho RM, Baptista A, Moura MC, Camilo ME, Rodrigues CM. Hepatocyte apoptosis, expression of death receptors, and activation of NF-kappaB in the liver of nonalcoholic and alcoholic steatohepatitis patients. *Am J Gastroenterol* 2004; **99**: 1708-1717
- 39 **Yajun Z**, Hongshan C, Baoxi S, Dengbing Y, Jianhua S, Xinsun G, Li Y, Yi C. Translocation of Bax in rat hepatocytes cultured with ferric nitrilotriacetate. *Life Sci* 2005; **76**: 2763-2772
- 40 **Obeng EA**, Boise LH. Caspase-12 and caspase-4 are not required for caspase-dependent endoplasmic reticulum stress-induced apoptosis. *J Biol Chem* 2005; **280**: 29578-29587
- 41 **Kroemer G**, Martin SJ. Caspase-independent cell death. *Nat Med* 2005; **11**: 725-730
- 42 **Alpy F**, Latchumanan VK, Kedingger V, Janoshazi A, Thiele C, Wendling C, Rio MC, Tomasetto C. Functional characterization of the MENTAL domain. *J Biol Chem* 2005; **280**: 17945-17952
- 43 **Foghsgaard L**, Wissing D, Mauch D, Lademann U, Bastholm L, Boes M, Elling F, Leist M, Jäättelä M. Cathepsin B acts as a dominant execution protease in tumor cell apoptosis induced by tumor necrosis factor. *J Cell Biol* 2001; **153**: 999-1010
- 44 **Liscum L**, Munn NJ. Intracellular cholesterol transport. *Biochim Biophys Acta* 1999; **1438**: 19-37

S- Editor Liu Y L- Editor Robert SE E- Editor Ma WH